The American Journal of Pathology, Vol. 171, No. 3, September 2007

DOI: 10.2353/ajpath.2007.070052

Neurobiology

Cholesterol Accumulation Is Associated with Lysosomal Dysfunction and Autophagic Stress in Npc1$^{-/-}$ Mouse Brain

Guanghong Liao,* Yueqin Yao,† Jihua Liu,† Zhang Yu,‡ Simon Cheung,* Ang Xie,* Xiaoli Liang,§ and Xiaoning Bi*

From the Department of Basic Medical Sciences, College of Osteopathic Medicine of the Pacific, Western University of Health Sciences, Pomona, California; the Department of Psychiatry and Human Behavior,† University of California Irvine, Irvine, California; the Electron Microscopy Core Laboratory,‡ Shanghai Medical College of Fudan University, Shanghai, China; and the Department of Pathology,§ Beijing Military Medical College, Beijing, China*

Niemann-Pick type C (NPC) disease is an autosomal recessive disorder caused by mutations of *NPC1* and *NPC2* genes. Progressive neurodegeneration that accompanies NPC is fatal, but the underlying mechanisms are still poorly understood. In the present study, we characterized the association of autophagic-lysosomal dysfunction with cholesterol accumulation in Npc1$^{-/-}$ mice during postnatal development. Brain levels of lysosomal cathepsin D were significantly higher in mutant than in wild-type mice. Increases in cathepsin D occurred first in neurons and later in astrocytes and microglia and were both spatially and temporally associated with intracellular cholesterol accumulation and neurodegeneration. Furthermore, levels of ubiquitinated proteins were higher in endosomal/lysosomal fractions of brains from Npc1$^{-/-}$ mice than from wild-type mice. Immunoblotting results showed that levels of LC3-II were significantly higher in brains of mutant than wild-type mice. Combined LC3 immunofluorescence and filipin staining showed that LC3 accumulated within filipin-labeled cholesterol clusters inside Purkinje cells. Electron microscopic examination revealed the existence of autophagic vacuole-like structures and multivesicles in brains from Npc1$^{-/-}$ mice. These results provide strong evidence that cholesterol accumulation-induced changes in autophagy-lysosome function are closely associated with neurodegeneration in NPC. *(Am J Pathol 2007, 171:962–975; DOI: 10.2353/ajpath.2007.070052)*

Niemann-Pick type C disease (NPC) is a fatal neurodegenerative disorder that mainly affects children. The pathological hallmark of NPC is the massive accumulation of cholesterol and other lipids in late endosomes and lysosomes.[1,2] In most cases (approximately 95%), the disease is caused by mutations in the *NPC1* gene[3] and the remainders by mutations in the *NPC2* gene; both genes encode proteins that play important roles in intracellular cholesterol transport.[4–6] Neurodegeneration in NPC shares a number of pathological features with those observed in Alzheimer's disease (AD), although the structures most affected in NPC are cerebellum and brainstem. Both diseases exhibit cholesterol metabolism impairment,[7–10] endosomal/lysosomal dysfunction,[5,8,11] and tauopathies.[12–15] Interestingly, the neurofibrillary tangles, the most common form of tauopathies, found in NPC are indistinguishable from those found in AD brains.[12,14] In both diseases, levels of free cholesterol are positively correlated with the incidence of intraneuronal neurofibrillary tangles.[16,17]

Several lines of evidence have established lysosomal dysfunction as an early-onset neuropathological feature of AD. Levels of lysosomal cathepsin D in neurons are increased in AD vulnerable regions before the onset of major pathology.[18] Cathepsin D up-regulation correlates on a cell-by-cell basis with other markers of early-stage AD, including decreased levels of the synaptic vesicular protein synaptophysin and increased levels of intraneuronal neurofibrillary tangles.[19,20] Experimentally induced lysosomal dysfunction is associated with rapid formation of neurofibrillary tangles in hippocampal slices cultured from apolipoprotein E knockout mice.[21] Cytoplasmic presence of cathepsin D can induce release of cytochrome *c* from mitochondria and activation of proapoptotic factors,

Supported by National Institute of Neurological Disorders and Stroke, National Institutes of Health grant NS048423, and by funds from Western University (to X.B.). X.B. was also supported by funds from the Daljit and Elaine Sarkaria Chair.

Accepted for publication May 15, 2007.

Address reprint requests to Dr. Xiaoning Bi, Department of Basic Medical Sciences, College of Osteopathic Medicine of the Pacific, Western University of Health Sciences, Pomona, CA 91766-1854. E-mail: xbi@westernu.edu.

which leads to caspase-dependent apoptosis, also referred to as type 1 programmed cell death.[22–24]

Lysosomes also participate in type 2 programmed cell death, referred to as autophagic cell death, which is defined by the presence of autophagic morphology.[25,26] Neuronal death with features of autophagy has been observed during normal development[27] and in pathological conditions, such as in AD[28,29] and in Parkinson's disease.[30] On the other hand, neuroprotective function of autophagy has also been implicated in certain neurodegenerative diseases, such as Huntington's disease. A recent study reported the existence of autophagic features in Purkinje cells in Npc1$^{-/-}$ mice.[31] To investigate further the roles of autophagy-lysosome system in neurodegeneration in NPC, the present study determined levels and localization of the lysosomal enzyme cathepsin D and of autophagic activity and the potential association of autophagic-lysosomal dysfunction with accumulation of cholesterol and neurodegeneration in brains of Npc1$^{-/-}$ mice.

Materials and Methods

Mice

Breeding pairs of BALB/cNctr-npc1^{NIH} mice heterozygous for Npc1 (+/−) were obtained from Jackson Laboratories (Bar Harbor, ME) and maintained in our animal facility in accordance with National Institutes of Health guidelines and protocols approved by the Institutional Animal Care and Use Committee with care to minimize distress to the animals. Mouse breeding and genotyping were performed as previously described.[32] Animals were sacrificed at postnatal weeks 1, 2, 4, and 8 (four to eight animals for each age group) under deep anesthesia (100 mg/kg sodium pentobarbital) by perfusion for immunohistochemical and histological studies or by decapitation for biochemical analyses. For histological studies, animals were perfused with phosphate-buffered saline (PBS) followed by 4% paraformaldehyde. Brains were removed and incubated with 15% sucrose followed by 30% sucrose before being sectioned at 25 μm with a microtome. Coronal sections were stored in a cryoprotective solution at −20°C before being processed for immunohistochemical studies.

Subcellular Fractionation

Brains from Npc1$^{-/-}$ and their wild-type littermates were dissected in ice-cold artificial cerebrospinal fluid and homogenized in homogenization buffer [homogenization buffer-EDTA: 3 mmol/L imidazole, 250 mmol/L sucrose, and 1 mmol/L ethylenediamine tetraacetic acid (EDTA), pH 7.4] containing protease inhibitors (Sigma-Aldrich, St. Louis, MO); homogenates were centrifuged for 10 minutes at 1500 × *g*. The sucrose concentration of the collected postnuclear supernatant was adjusted to 40.6% by the slow addition of 62% sucrose in homogenization buffer-EDTA. Postnuclear supernatant was then carefully overloaded with 1.5 ml of 35% and 1.0 ml of 25% sucrose in homogenization buffer-EDTA, and the samples were centrifuged in an SW 55 rotor (Beckman Instruments, Inc., Palo Alto, CA) at 14,000 × *g* for 90 minutes at 4°C. Subcellular fractions were collected from the top of the tube. The late endosome/lysosome-enriched fraction was localized in the upper interface, containing 25% sucrose and homogenization buffer, and the early endosome-enriched fraction in the middle interface containing 35 and 25% sucrose. The lower interface containing 40.6 to 35% sucrose was enriched in plasma membranes and other heavy membrane compartments.

Western Blots

Electrophoresis and immunoblotting were performed following conventional procedures. In brief, after protein concentration was determined, proteins (40 to 60 μg) of postnuclear supernatant from different brain regions [cerebellum, brainstem (including interbrain, midbrain, and hindbrain), hippocampus, and cortex] or of other subcellular fractions were denatured by boiling for 5 minutes in a sample buffer (2% sodium dodecyl sulfate, 50 mmol/L Tris-HCl pH 6.8, 10% 2-mercaptoethanol, 10% glycerol, and 0.1% bromphenol blue) and separated by electrophoresis on sodium dodecyl sulfate-polyacrylamide gels (12%), after which proteins were transferred to nitrocellulose membranes. Nitrocellulose membranes were incubated with primary antibodies for 12 to 16 hours at 4°C; immunoreactivity was visualized by using enhanced chemiluminescence (ECL Plus kit and reagents; Amersham Pharmacia Biotech, Piscataway, NJ). Antibodies used included anti-cathepsin D (1:1000; EMD Biosciences, San Diego, CA), anti-cathepsin B (1:100; Santa Cruz Biotechnology, Santa Cruz, CA), anti-rab7 (1:1000; Santa Cruz Biotechnology), anti-ubiquitin (1:500; Zymed, Carlsbad, CA), and anti-LC3 serum (gift from T. Yoshimori, National Institute of Genetics, Mishima, Shizuoka, Japan[33]). Levels of different bands were analyzed by using the National Institutes of Health Image program (Bethesda, MD). Statistical significance was determined by two-tailed Student's *t*-test.

Activity Assay of Cathepsins B and D

Whole homogenates of brainstem, cerebellum, or hippocampus from Npc1$^{-/-}$ and wild-type mice were used to analyze the activity of cathepsins B and D using fluorogenic immunocapture activity assay kits (EMD Biosciences) according to the kit instructions.

Immunohistochemistry

Sagittal sections from cerebellum and coronal sections from the rest of the brain of animals from different ages were simultaneously processed for immunostaining. Immunohistochemistry was performed using the avidin-biotin horseradish peroxidase complex method. In brief, free-floating sections were first incubated in 10% normal horse serum (for monoclonal antibodies) or 3% normal goat serum (for polyclonal antibodies) diluted in PBS with 0.1% Triton X-100 for 1 hour at room temperature, fol-

lowed by incubation with primary antibodies overnight at 4°C. Antibodies used were anti-cathepsin D (1:500; EMD Biosciences) and anti-cathepsin B (1:100; Santa Cruz Biotechnology). After three washes in PBS, sections were incubated with corresponding biotinylated secondary antibodies (1:400; Vector Laboratories, Burlingame, CA) in 5% normal horse serum or 1.5% normal goat serum solution for 2 to 3 hours, then in avidin-biotin horseradish peroxidase complex diluted in PBS for 45 minutes. Peroxidase reaction was performed with 3,3′-diaminobenzidine tetrahydrochloride (0.05% in 50 mmol/L Tris-HCl buffer, pH 7.4) as chromogen and 0.03% H_2O_2 as oxidant. Free-floating sections were mounted on precoated slides (SuperPlus; Fisher Scientific International Inc.) and air-dried. Sections were then dehydrated in graded ethanol and finally covered with Permount (Fisher Scientific).

Double-labeling immunohistochemistry was done with sections first incubated with primary antibodies [rabbit anti-cathepsin D in combination with either rat anti-F4/80 (1:1000; Serotec, Raleigh, NC) or mouse anti-calbindin (1:1000; Abcam, Cambridge, MA)], then with corresponding secondary antibodies conjugated with Alexa Fluor 488 or Alexa Fluor 594. Both secondary antibodies were purchased from Molecular Probes, Eugene, OR.

Filipin Staining

Filipin has been demonstrated to specifically stain free cholesterol because treatment with cholesterol oxidase results in a complete loss of fluorescence.[34] Brain tissue sections were washed with phosphate-buffered saline and incubated in the dark with 125 μg/ml filipin in PBS for 3 hours under agitation at room temperature. After washing in PBS, some sections were further processed for immunostaining with anti-calbindin or -LC3 (1:3000; Abgent, San Diego, CA) antibodies and corresponding secondary antibodies conjugated with Alexa Fluor 594.

Images of immunostained sections from different brain regions were visualized using a Zeiss microscope (Axioskop 2 Mot Plus) and digitized via a Zeiss digital photo camera (AxioCam Hrc) and the Axiovision program, version 3.1 (Zeiss), was used to capture and save digitized images. Digitized images were then assembled in Photoshop (version 7; Adobe Systems, Mountain View, CA) with only the brightness adjusted to match other panels in a given figure. Images of double fluorescent labeled sections were acquired by using a Nikon confocal microscope (Nikon TE 2000U with D-Eclipse C1 system; Melville, NY).

Electron Microscopy Analysis

Electron microscopy analysis was performed as previously described.[35] In brief, animals were perfused with an ice-cold solution of 0.1 mol/L phosphate buffer, pH 7.4, containing 1.5% paraformaldehyde and 1.5% glutaraldehyde. Cerebellum blocks were transferred to 2.5% glutaraldehyde in 0.1 mol/L phosphate buffer, pH 7.4, at 4°C for 24 hours, rinsed overnight in the phosphate buffer, postfixed with 1% osmium tetroxide in phosphate buffer for 2 hours, followed by dehydration and embedded in epoxy resin. Ultrathin sections were prepared using a Reichert ultramicrotome, contrasted with uranyl acetate and lead citrate, examined under a Philips CM120 transmission electron microscope at 80 kV.

Results

Increased Levels of Cathepsin D in Brains of Npc1$^{-/-}$ Mice during Postnatal Development

Cathepsin D is synthesized as an inactive 52- to 53-kd proenzyme; cathepsin D activation produces a 48-kd (single chain) intermediate and mature forms at 34 and 14 kd (heavy and light chains, respectively).[36,37] Immunoblotting studies using anti-cathepsin D antibodies revealed an early-onset increase in levels of cathepsin D (both single chain and heavy chain) in all brain regions tested. At 2 weeks postnatal, levels of single chain cathepsin D (Figure 1A, arrows) in brainstem, cerebellum, cerebral cortex, and hippocampus of Npc1$^{-/-}$ mice were 274 ± 7%, 190 ± 5%, 176 ± 12%, and 199 ± 5% of those measured in Npc1$^{+/+}$ mice, respectively (means ± SEM, $n = 5$, $P < 0.001$; Figure 1B). Levels of single chain-cathepsin D remained elevated at 4 weeks with further increase being only evident in cerebellum (Figure 1B). Changes in heavy chain-cathepsin D (Figure 1A, −) were similar to those observed for the single chain isoform (Figure 1, A and B).

Immunohistochemical results revealed significant increases in cathepsin D immunoreactivity throughout the brain in 1-week-old Npc1$^{-/-}$ mice. In contrast to the pattern observed in wild-type mice, numerous darkly labeled cells were found in cerebellum of Npc1$^{-/-}$ mice, and most of them were located in white matter (compare Figure 2, B with A), suggesting that they were glial cells. High magnification examination showed that cathepsin D immunoreactivity was also moderately increased in Purkinje cells in Npc1$^{-/-}$ (Figure 2D) compared with wild-type mice (Figure 2C). The number of cathepsin D-immu-

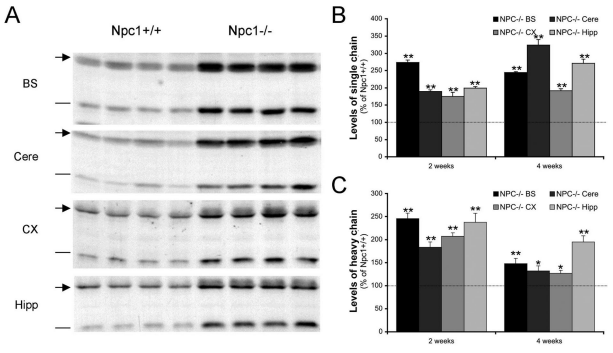

Figure 1. Cathepsin D levels in brain of Npc1$^{+/+}$ and Npc1$^{-/-}$ mice during postnatal development. **A:** Representative images of blots of samples from 2-week-old animals labeled with anti-cathepsin D antibodies. **Arrows** correspond to the "single chain" isoform of cathepsin D, whereas lines indicate the "heavy form" of cathepsin D (see Results for details). **B** and **C:** Quantitative results for levels of single chain cathepsin D and heavy chain cathepsin D isoforms, respectively. Data are presented as percentage of values from Npc1$^{+/+}$ mice and are means ± SEM. $n = 5$; $^{*}P < 0.05$, and $^{**}P < 0.01$.

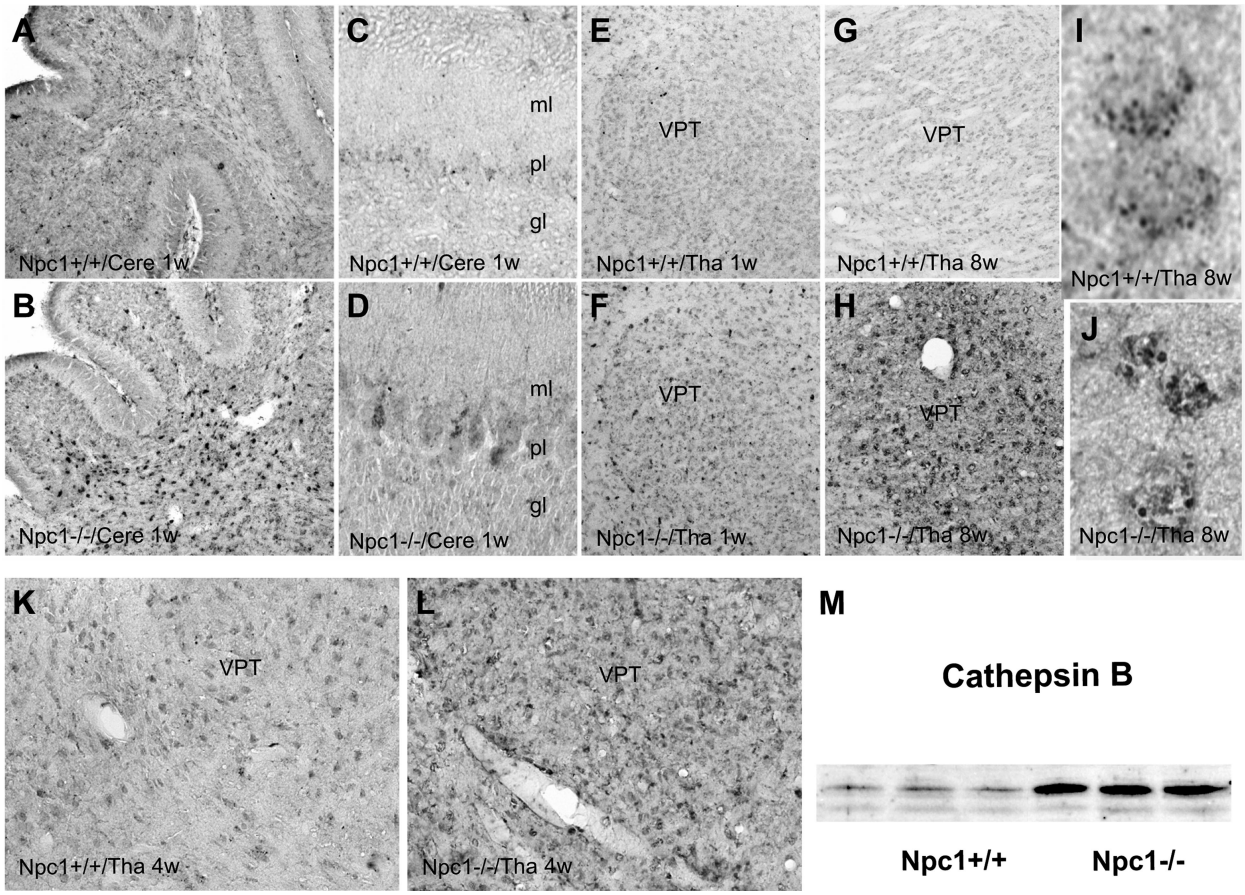

Figure 2. Distribution of cathepsin D and B in cerebellum and thalamus of Npc1$^{-/-}$ mice during postnatal development. Cerebellar (**A–D**) and thalamic (**E–L**) tissue sections were prepared from Npc1$^{+/+}$ (**A**, **C**, **E**, **G**, **I**, and **K**) and Npc1$^{-/-}$ (**B**, **D**, **F**, **H**, **J**, and **L**) mice at postnatal week 1 (**A–F**), 4 (**K** and **L**), and 8 (**G–J**) and were immunostained with anti-cathepsin D (**A–J**) or anti-cathepsin B (**K** and **L**) antibodies. Higher magnification images show that in Npc1$^{+/+}$ mice (**I**) cathepsin D immunoreactive products are mainly located in small-sized granules, whereas in Npc1$^{-/-}$ mice they are present in larger puncta and their surrounding cytoplasmic structures (**J**). **M** shows immunoblots of cathepsin B-labeled samples from brainstem of 4-week-old mice. ml, molecular layer; pl, Purkinje layer; gl, granular layer; VPT, ventral posterior nucleus of thalamus. Scale bar = 50 μm (**A** and **B**); 12.5 μm (**C–H** and **K** and **L**).

noreactive cells was also increased in the ventral posterior nuclei of the thalamus at 1 week (Figure 2F) compared with that in Npc1$^{+/+}$ mice (Figure 2E), and it was further increased by 4 weeks. By 8 weeks, the ventral posterior nuclei of the thalamus were filled with anti-cathepsin D-immunopositive cells (Figure 2H). Higher magnification images showed that although cathepsin D-immunoreactive products existed in small granules that were scattered in cell bodies in the ventral posterior nuclei of the thalamus of Npc1$^{+/+}$ mice (Figure 2I), those in Npc1$^{-/-}$ mice were present in larger punctates that often clustered together (Figure 2J). Furthermore, higher cytoplasmic levels of cathepsin D immunoreactivity were observed around these punctates. Immunohistochemical and immunoblotting results showed that levels of another lysosomal hydrolase, cathepsin B, were also increased in mutant mice as compared with wild-type mice (Figure 2, K–M). Cathepsin D activity in homogenates from brainstem of 4-week-old Npc1$^{-/-}$ mice was about 2.4 times higher than that from Npc1$^{+/+}$ mice (n = 3 for Npc1$^{+/+}$ and n = 4 for Npc1$^{-/-}$ mice; $P < 0.01$). Cathepsin B activity also increased in samples from hippocampus (295 ± 8%; $P < 0.01$) and cerebellum (187 ± 3%; $P < 0.01$) of 8-week-old Npc1$^{-/-}$ mice (n = 5) compared with Npc1$^{+/+}$ mice (n = 5).

Double immunofluorescence staining was used to determine the cellular and subcellular localization of cathepsin D in mutant mice. At 4 weeks, cathepsin D-immunoreactive granules were observed in cell bodies of calbindin-immunopositive Purkinje cells in Npc1$^{-/-}$ mice (Figure 3A, the asterisk in bottom panels), whereas very few cathepsin D positive granules were found in the cerebellum of Npc1$^{+/+}$ mice (Figure 3A, top panels). In the cerebellum of 4-week-old Npc1$^{-/-}$ mice, cathepsin D immunoreactivity was also found in reactive microglia identified with antibodies against the macrophage marker F4/80 antigen (data not shown). By 8 weeks, cathepsin D-labeled granules accumulated mainly in the apical processes of small cells dispersed among Purkinje cells in wild-type mice; from their position and morphology, these cells resembled Bergman glia (Figure 3B, arrows). Cathepsin D immunoreactivity in Bergmann glia in Npc1$^{-/-}$ mice was similar to that in wild-type mice (Figure 3B). In the cerebellum of 8-week-old Npc1$^{-/-}$ mice, cathepsin D immunoreactivity was also observed in F4/80-labeled reactive microglia (Figure 3B, mg); at this postnatal

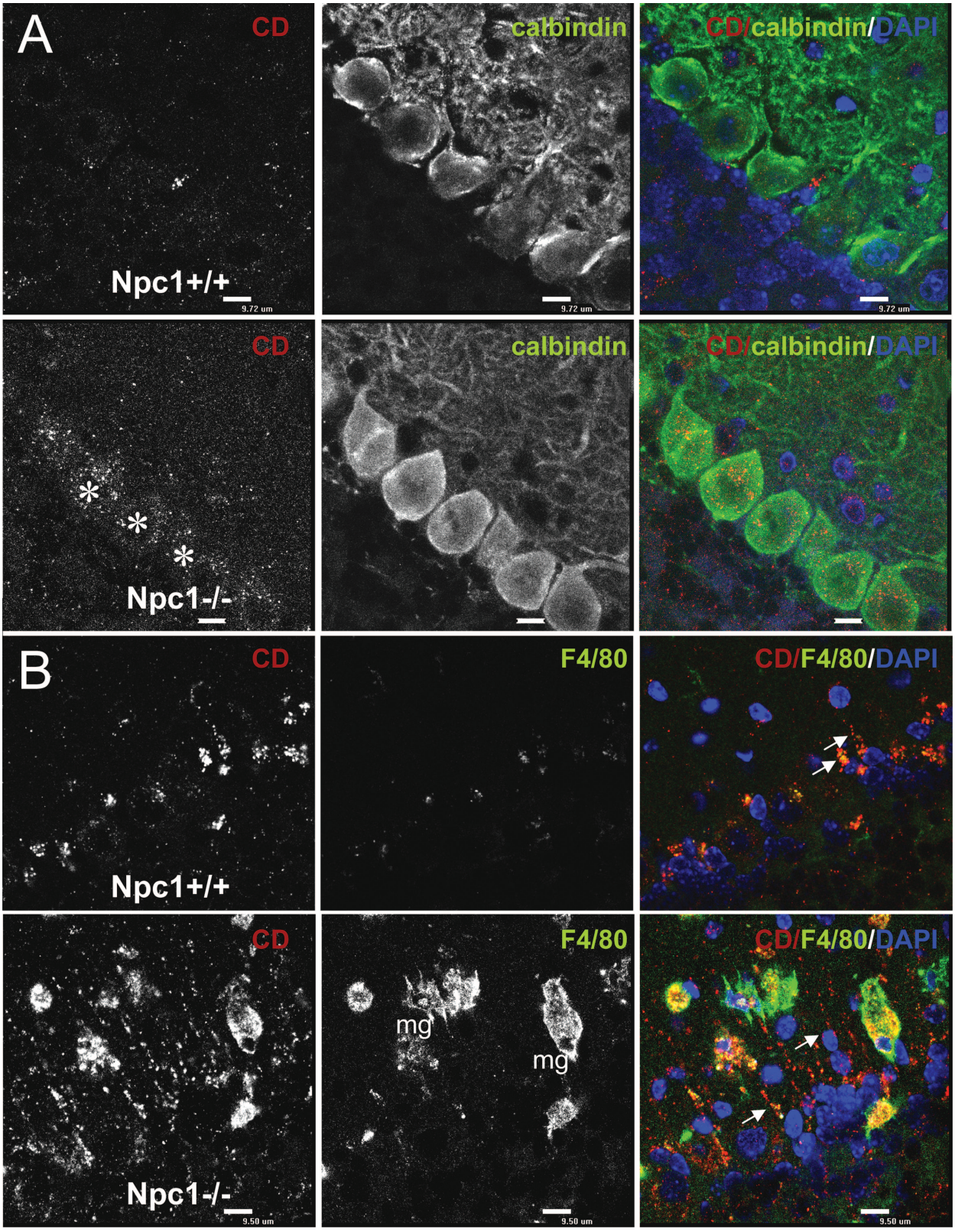

Figure 3. Cellular localization of cathepsin D in cerebellar cortex at 4 and 8 weeks postnatal. **A:** Double immunofluorescence staining using antibodies against cathepsin D (red) and calbindin (green) in cerebellum of 4-week-old $Npc1^{+/+}$ (top panels) and $Npc1^{-/-}$ (bottom panels) mice. DAPI (blue) was included in the mounting medium to label nuclei. **B:** Double immunofluorescence staining using antibodies against cathepsin D (red) and F4/80 (green; a marker for microglia) in cerebellum of 8-week-old $Npc1^{+/+}$ (top panels) and $Npc1^{-/-}$ (bottom panels) mice. *, Purkinje cells; **arrows**, Bergmann glia; mg, microglia. Scale bar = 10 μm.

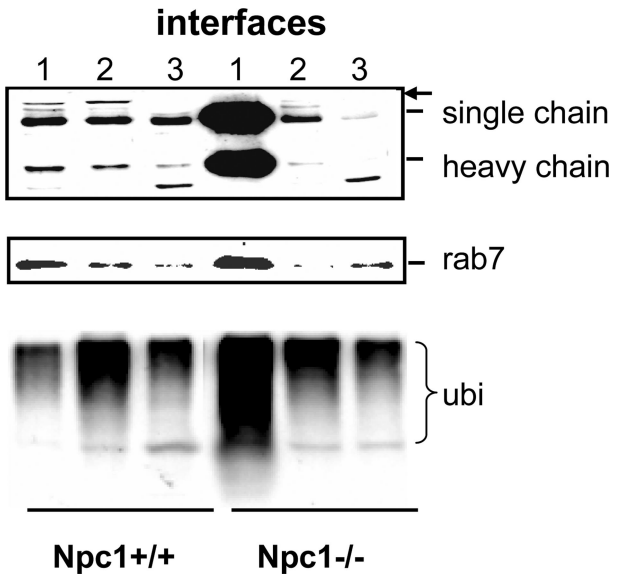

Figure 4. Abnormal protein distribution and ubiquitination in brain of Npc1$^{-/-}$ mice. Immunoblots of samples from different fractions labeled with anti-cathepsin D [single chain and heavy chain] and pro-cathepsin D (**arrow** in top panel), -rab7 (middle panel), or -ubiquitin (ubi, bottom panel) antibodies. Note the marked increase in cathepsin D in fraction 1 in samples from Npc1$^{-/-}$ mice. Note also the marked increase in levels of ubiquitinated proteins in endosomal/lysosomal fraction in the mutant mice. Interface 1 contains membrane from late endosome/lysosomes, interface 2 contains mainly early endosomes, and interface 3 contains other membrane structures. Western blots of subcellular fractions are representative of two experiments; each included four animals from each genotype. The results were very similar in both experiments.

age, microglia became larger and rounder and invaded both the Purkinje cell layer and the molecular layer.

Abnormal Subcellular Protein Distribution in Brains of Npc1$^{-/-}$ Mice

The subcellular localization of various proteins was determined by combining subcellular fractionation and immunoblotting analysis. Cathepsin D levels were markedly higher in the late endosomal/lysosomal fractions in mutant compared with wild-type mice (Figure 4, top panel). Levels of the small GTP-binding protein Rab7, which participates in the maturation of autophagic vacuoles,[38,39] were higher in the late endosomal/lysosomal fractions but lower in the early endosomal fractions in Npc1$^{-/-}$ compared with wild-type mice. As a close link between autophagy and protein ubiquitination has previously been reported,[40,41] levels of ubiquitinated proteins in different subcellular fractions were determined by immunoblotting using anti-ubiquitin antibodies. Proteins residing in the late endosomal/lysosomal fractions were highly ubiquitinated (Figure 4, bottom panel). Ubiquitin immunoreactive products were smeared from the top to the middle part of the gel resulting in a typical staining pattern that generally implies polyubiquitination.

Increased Levels of the Mammalian Autophagic Protein LC3-II in Brains of Npc1$^{-/-}$ Mice

Lysosomal dysfunction perturbs normal protein degradation and amino acid recycling, which could result in

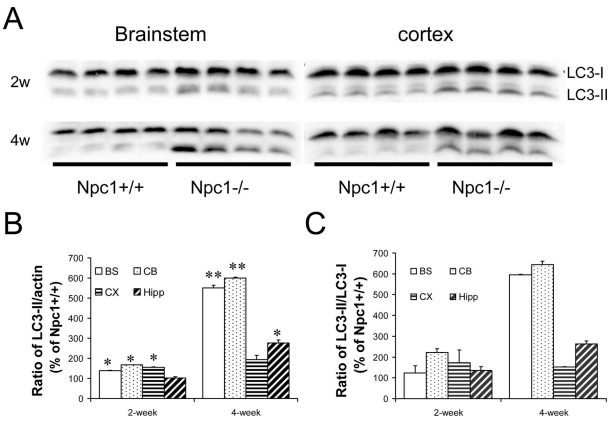

Figure 5. LC3-II levels in brains of Npc1$^{-/-}$ mice during postnatal development. **A:** Representative images of blots labeled with anti-LC3 serum. Levels of LC3-II (**B**) and the ratio of LC3-II/LC3-I (**C**) are higher in mutant mice, especially in brainstem (BS) and cerebellum (CB); moderate increases were observed in cortex (CX) and hippocampus (Hipp). Data are presented as percentage of values from Npc1$^{+/+}$ mice and are means ± SEM. $n = 4$; $^{*}P < 0.05$, and $^{**}P < 0.01$.

a state of "cellular amino acid starvation," the most common cause of autophagy. To determine the status of autophagic activity in brains of Npc1$^{-/-}$ mice, levels of the microtubule-associated protein 1 light chain 3 (LC3), a mammalian homologue of the yeast autophagic protein Atg8, were assessed in various brain regions by immunoblotting. Like Atg8, LC3 is modified via a ubiquitination-like system[33,42]; LC3 is first cleaved in its carboxyl terminal and becomes LC3-I, which is further modified by Atg7 and Atg3 into a membrane-bound form, LC3-II.[42] Modification of LC3 is essential for the formation of autophagosomes; thus LC3-II has been widely used as an autophagosomal marker.[33] Although brain levels of LC3-I in mutant mice did not significantly differ from that in wild-type mice, levels of LC3-II in 2-week-old mutant mice were significantly higher than those in wild-type mice (Figure 5). This difference was even greater in 4-week-old animals. Interestingly, elevation of LC3-II was more prominent in areas that are more sensitive to NPC-type injury. The LC3-II/LC3-I ratio exhibited similar changes as those of LC3-II in brain of Npc1$^{-/-}$ mice compared with those in wild-type mice, further confirming that only LC3-II was altered.

Combined calbindin immunofluorescence and filipin staining confirmed that at postnatal week 4, accumulation of cholesterol in the cerebellum was mainly in Purkinje cells (Figure 6A, arrows in bottom panels). Combined LC3 immunofluorescence and filipin staining showed that although there was virtually no LC3 immunopositive granules in wild-type mice at 4 weeks, occasional LC3-immunopositive clusters were found in the apical dendrites of Purkinje cells filled with filipin-labeled free cholesterol in Npc1$^{-/-}$ mice (data not shown). Interestingly, by 8 weeks LC3 immunopositive granules were found scattered in the soma of Purkinje cells in wild-type mice (Figure 6B, top panels), whereas in mutant mice, smaller LC3 granules aggre-

gated with cholesterol clusters at one pole of Purkinje cells (Figure 6B, asterisks in bottom panels) or in some

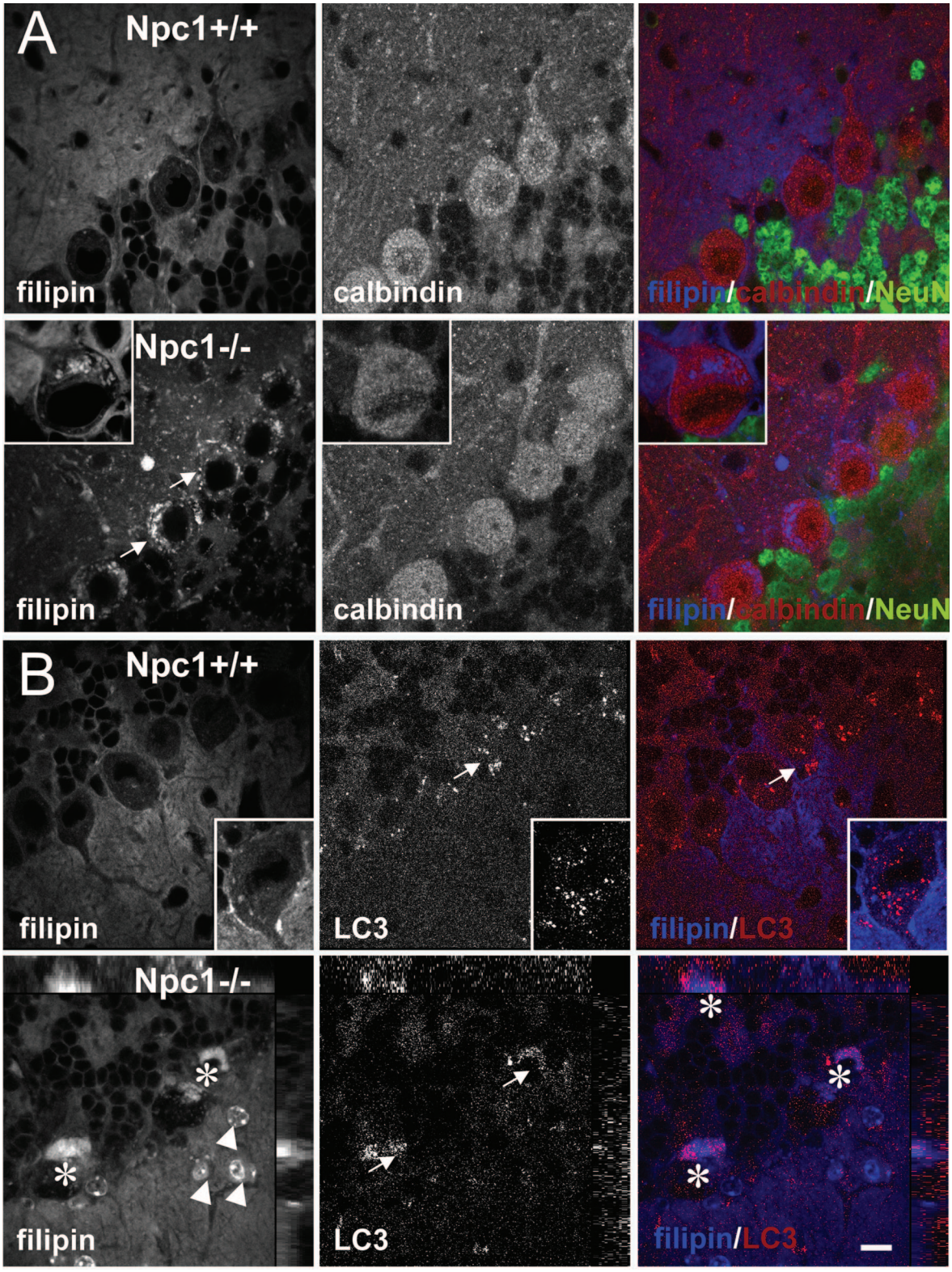

Figure 6. Cholesterol accumulation and sequestration of LC3 in Purkinje cells in Npc1$^{-/-}$ mice. **A:** Localization of filipin-stained free cholesterol (blue) in calbindin-immunopositive Purkinje cells (red) in cerebellum from 4-week-old Npc1$^{+/+}$ (top) and Npc1$^{-/-}$ (bottom) mice. Note the accumulation of cholesterol in Purkinje cells in mutant mice but not in wild-type mice. Anti-NeuN (green) was used to label neurons. **B:** Combined LC3 immunostaining (red) with filipin staining (blue) in 8-week-old Npc1$^{+/+}$ (top) and Npc1$^{-/-}$ (bottom) mice. Top panels show LC3-positive puncta present in Purkinje cells of 8-week-old Npc1$^{+/+}$ mice; **inset** is a higher magnification image showing the subcellular distribution of LC3 puncta. Bottom panels show three-dimensional colocalization of LC3 with cholesterol in Purkinje cells of an 8-week-old mutant mouse. Scale bar = 10 μm.

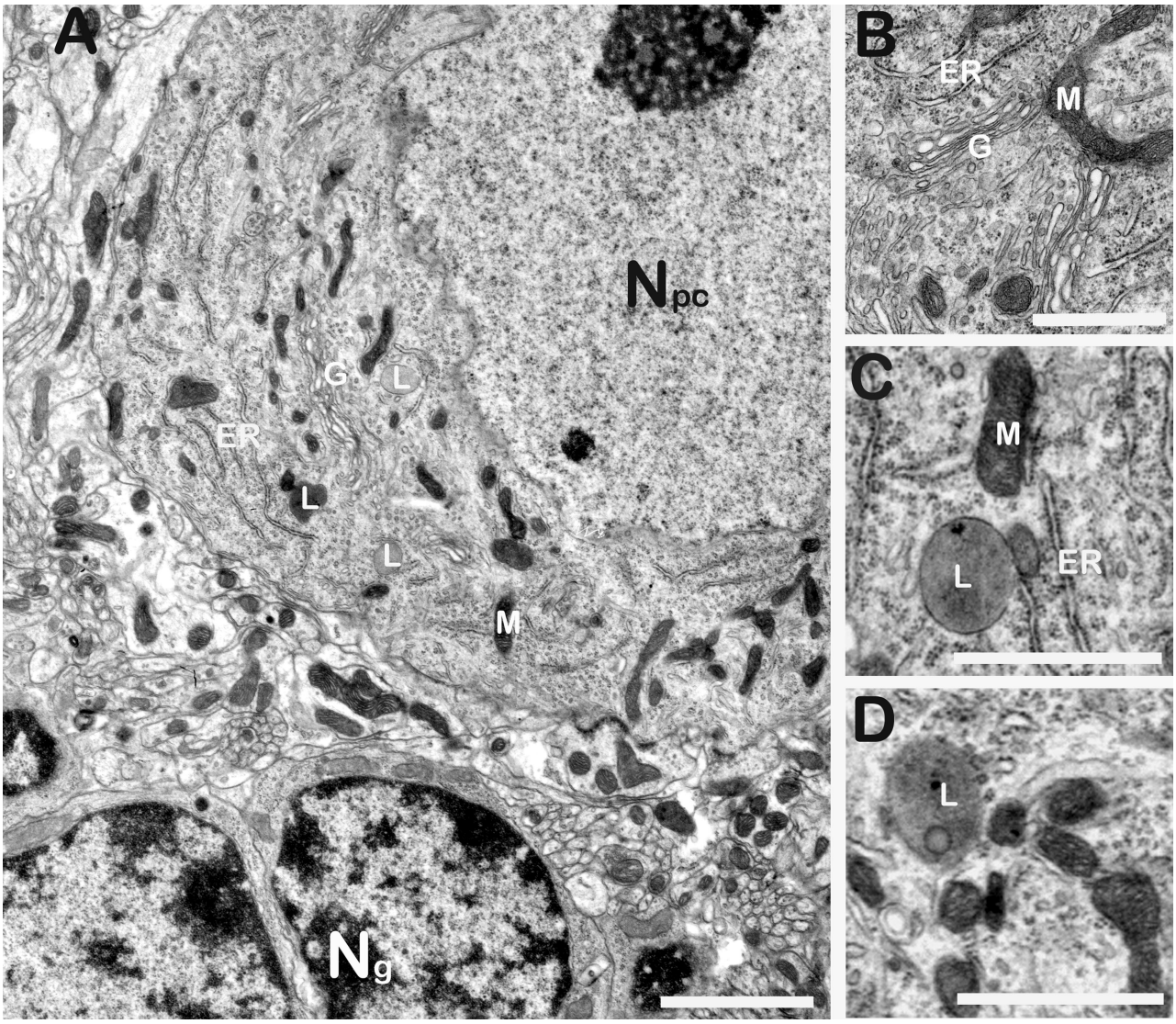

Figure 7. Ultrastructure of Purkinje cells in Npc1$^{+/+}$ mice. **A:** A Purkinje cell in the vicinity of granule cells in a 6-week-old Npc1$^{+/+}$ mouse. **B:** Stacks of Golgi apparatus are present in a Purkinje cell. **C** and **D:** Lysosome-like structures exist in Purkinje cells. ER, endoplasmic reticulum; G, Golgi apparatus; L, lysosome; M, mitochondria; Ng, nucleus of granule cell; Npc, nucleus of Purkinje cell. Scale bars = 2 μm (**A**); 1 μm (**B–D**).

densely packed small cells. Colocalization of LC3 with cholesterol was confirmed by orthogonal three-dimensional analysis of individual Purkinje cells (Figure 6B).

Ultrastructural Changes in Brains of Npc1$^{-/-}$ Mice

As ultrastructural examination by transmission electron microscopy remains the most convincing and standard method to detect autophagy,[43] the morphology of intracellular inclusions in brain of Npc1$^{-/-}$ mice was further evaluated by electron microscopy. Purkinje cells in the cerebellum of 6-week-old wild-type mice had a centrally located nucleus (Figure 7A) with stacks of perinuclear Golgi complex (Figure 7, A and B), polyribosomes, rough endoplasmic reticulum and mitochondria that were distributed relatively evenly in the cytoplasm (Figure 7). Spherical or oval-shaped lysosomes (Figure 7, A, C, and D) were also observed in the cytoplasm of Purkinje cells in wild-type mice. Electron microscopy analysis of Purkinje cells from 6-week-old Npc1$^{-/-}$ mice revealed a different feature: numerous intracellular inclusion bodies with different sizes and shapes accumulated in one side of the cell body and pushed a kidney-shaped nucleus to the other side (Figure 8A) and a cluster of endoplasmic reticulum and mitochondria aggregated along the indent side of the nucleus. High-magnification images showed that these inclusion bodies were mostly membranous vacuoles with double membranes (arrowheads) or multilamellated electron-dense material (Figure 8, arrows). In addition, abnormal multivesicular profiles (Figure 8) similar to the polymembranous cytoplasmic bodies described in human NPC disease were also common. Interestingly, lysosome-like structures with homogeneous filling of moderate levels of electron-dense materials, as those observed in wild-type mice, seemed to dis-

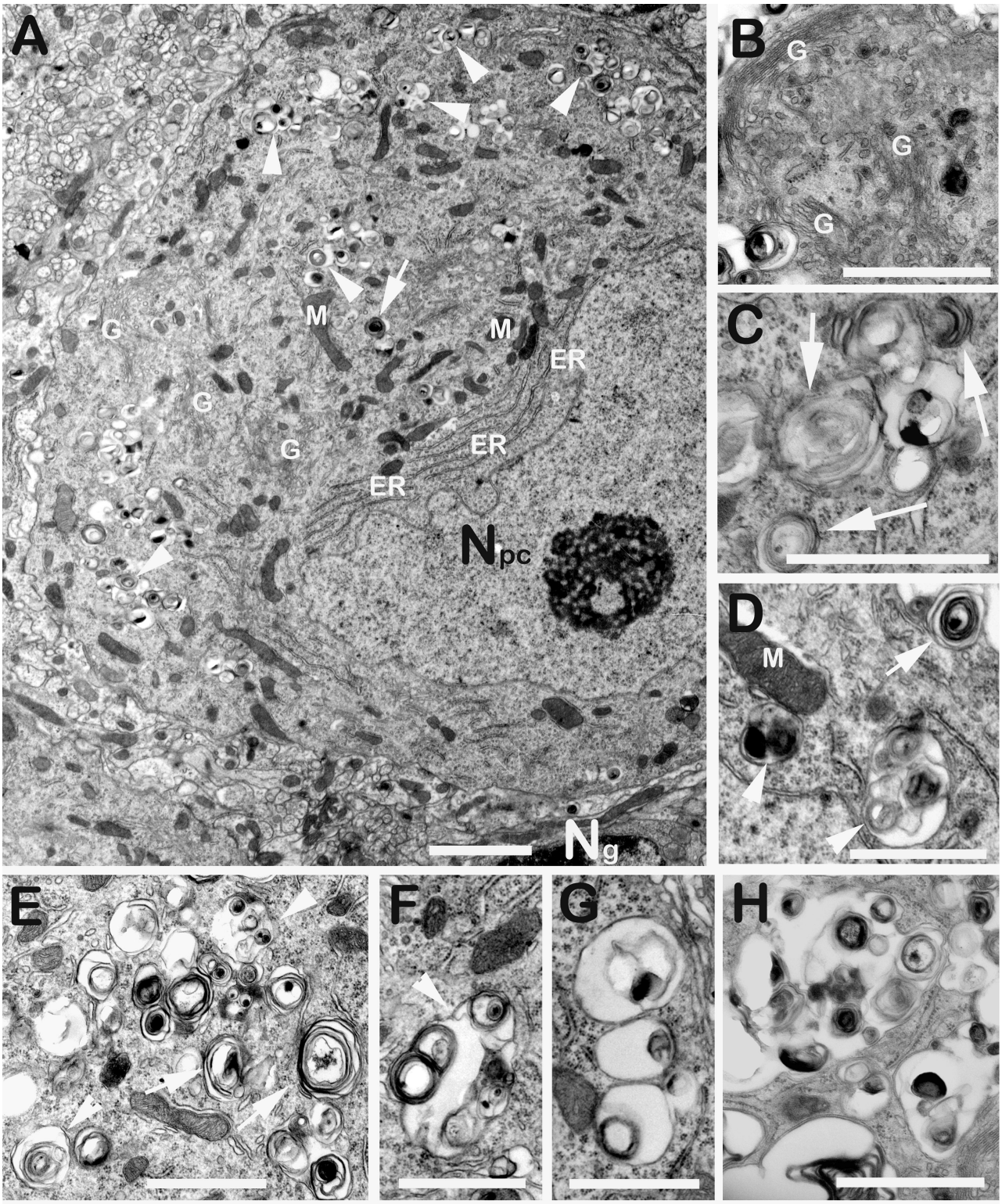

Figure 8. Ultrastructure of Purkinje cells in Npc1$^{-/-}$ mice. **A:** A Purkinje cell in a 6-week-old Npc1$^{-/-}$ mouse. Numerous vacuoles (**arrowheads**) of different sizes with various levels of electron-dense materials are present in the cytoplasm. **B:** Stacks of Golgi apparatus are clustered in the cytoplasm. **C–H:** Morphology of various membranous vacuoles. Some of them are with double membranes (**arrowheads**), whereas others have multilamellated structures (**arrows**). Scale bars = 2 μm (**A**); 1 μm (**B–H**).

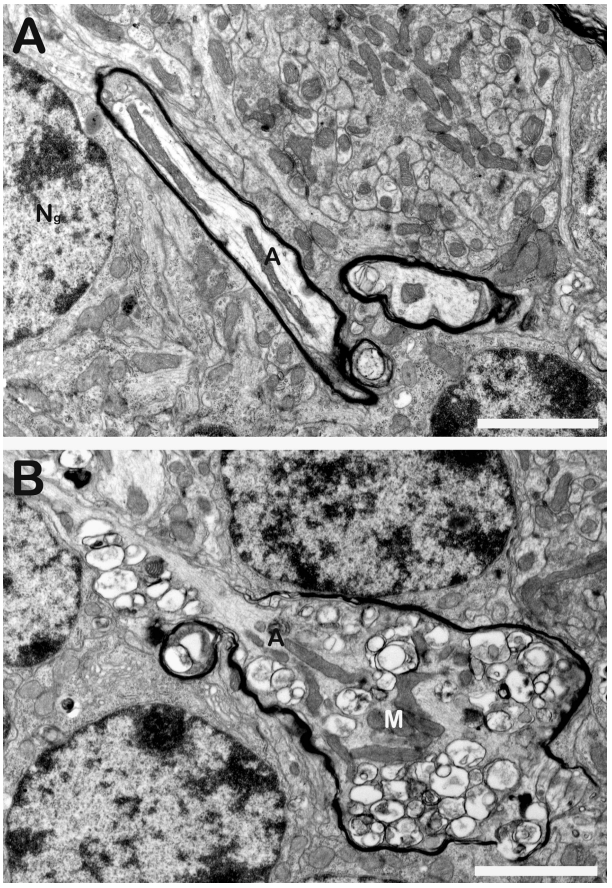

Figure 9. Axonal pathology in Npc1$^{-/-}$ mice. **A:** A myelinated axon of a Purkinje cell axon exists in the vicinity of two granule cells in a 6-week-old wild-type mouse. **B:** An axonal spheroid in a myelinated Purkinje cell axon is located among granule cells in a 6-week-old Npc1$^{-/-}$ mouse. Note that a cluster of mitochondria is surrounded by vacuoles accumulated within the spheroid. Scale bars = 2 μm.

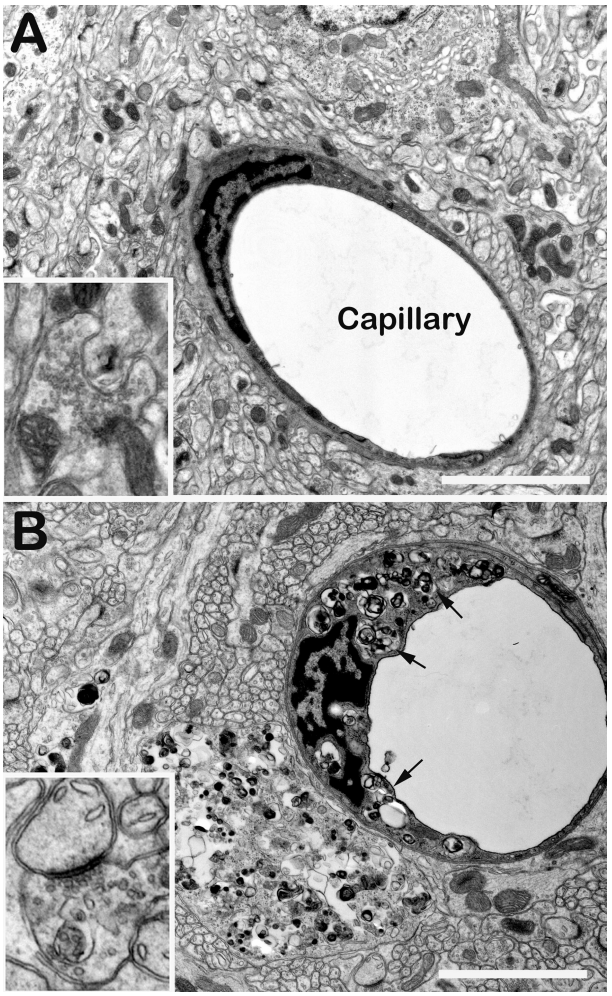

Figure 10. Capillary pathology in cerebellum of Npc1$^{-/-}$ mice. A capillary is surrounded by parallel fibers and synapses in the cerebellum of a 6-week-old wild-type (**A**) or a mutant (**B**) mouse. Note the membranous inclusions in the endothelial cell in the mutant mouse. **Insets** show synapses. Scale bars = 2 μm.

appear in mutant mice. Aggregation of membranous vacuoles was also observed in myelinated Purkinje cell axons that were located among granule cells; these vacuoles clustered with mitochondria and formed axonal spheroids (Figure 9B). Finally, membranous vacuoles were also observed in endothelia in capillaries located among parallel fibers and numerous synapses (compare Figure 10, B to A).

Discussion

Early-Onset Lysosomal Abnormality May Contribute to Neurodegeneration in Npc1$^{-/-}$ Mice

Results from the present study indicated that abnormal levels of the lysosomal enzyme cathepsin D occurred early during postnatal development in Npc1$^{-/-}$ mouse brain. Increases in levels of both single chain and heavy chain cathepsin D isoforms were clearly detected by immunoblotting in all brain areas examined at 2 weeks postnatal. Both isoforms possess catalytic activities,[36,37] suggesting that cathepsin D activity might be increased in these areas in mutant mice. Indeed, enzymatic assay confirmed that cathepsin D activity was increased in the brainstem. Likewise, activity of another lysosomal hydrolase, cathepsin B, was also increased in the brains of mutant mice. However, the highest increases in cathepsin D levels were observed in the brainstem and cerebellum, two regions that exhibit early and marked neurodegeneration. Immunohistochemistry analyses indicated that increases in cathepsin D occurred both in neurons and in glial cells; dense cathepsin D immunoreactivity was observed in the soma of Purkinje cells of Npc1$^{-/-}$ mice by 2 weeks postnatal, whereas clear glial localization was prominent in several brain regions at 4 weeks, results which are in agreement with those reported in an earlier study[44] and with the early-onset inflammatory response we previously reported.[32] Enhanced cathepsin D immunostaining occurred mainly in brain structures exhibiting both accumulation of intracellular free cholesterol and neurodegeneration. Double immunofluorescence analysis showed that enhanced cathepsin D was present in both neurons and glia at 4 weeks but mainly in glial elements by 8 weeks postnatal.

Increases in number of secondary lysosomes and changes in levels of lysosomal enzymes have previously been associated with brain aging and age-related neurodegeneration.[45] In particular, increased cathepsin D levels occur in AD brains before the onset of major pathology, and this was correlated on a cell-by-cell basis with decreases in synaptic proteins and with the presence of one of the disease's hallmarks, neurofibrillary tangles.[19,20] Furthermore, pharmacological suppression of cathepsins B and L resulted in increase in cathepsin D,[46,47] lysosomal proliferation, formation of meganeurites (axon swellings that were often located proximal to the cell body) in cultured rat hippocampal slices,[35,48] and in tau hyperphosphorylation and generation of neurofibrillary tangles in cultured hippocampal slices from apolipoprotein E-deficient mice.[21] Furthermore, the compromise of lysosomal membrane and subsequent leakage of cathepsin D into cytoplasm are early events in amyloid β peptide treatment-induced cell death in cultured hippocampal neurons.[49] These results have supported the hypothesis that lysosomal dysfunction contributes to AD-type neuropathologies. A recent study from Nixon's laboratory[29] showed that extensive macroautophagy might contribute to changes in lysosomal function in AD. Thus our results further expand the previously noted similarities in neuropathological mechanisms between NPC and AD and suggest therefore that lysosomal dysfunction may contribute to NPC type neurodegeneration.

Abnormal Autophagic Activity and Protein Ubiquitination in Brains of Npc1$^{-/-}$ Mice

Impairment in cholesterol transport induced by NPC1 mutations is associated with abnormal vesicle trafficking and redistribution of presenilin,[50] glycosphingolipids,[51] rab7,[52,53] and annexin II,[54] although the underlying mechanism has remained elusive. Immunoblotting analysis revealed an early-onset increase in levels of LC3-II, a widely used marker for autophagy. Levels of this protein were particularly high in the brainstem and cerebellum, two brain regions exhibiting the severest neuronal death, which suggests that autophagy may contribute to neurodegeneration. Increases in autophagic stress were further confirmed by ultrastructural detection of autophagosome-like vacuoles that were prominent in brains of Npc1$^{-/-}$ animals but uncommon in wild-type mice, findings that are consistent with results from a recent report.[31] We previously showed that levels of inactive GSK-3β were markedly increased in Npc1$^{-/-}$ mouse brains and this increase was closely associated with inactivation of nuclear factor κB signaling in brains of Npc1$^{-/-}$ mice during early development.[55] Sequestration of GSK-3β by autophagy may contribute to inhibition of this kinase, which also explains the predominant lysosomal location of the enzyme.[55] Relocation of GSK-3 to lysosomes could also result from enhanced chaperone-mediated autophagy, a possibility that needs to be further explored. It has previously been reported that, although GSK-3β was located predominantly in the cytosol of SH-SY5Y cells, its active form was disproportionately higher in nuclei and mitochondria.[56] The active form of another kinase, extracellular signal-regulated kinase 1/2, was also localized in the mitochondria and autophagosomes in Lewy body disease.[57] It is conceivable that changes in subcellular localization of these kinases could alter their activities; however, further experiments are needed to clarify this issue. Interestingly, proteins in the late endosomal/lysosomal fractions of brains from Npc1$^{-/-}$ mice were also highly ubiquitinated. Protein ubiquitination, a type of post-translational protein modification, is generally used to deliver targeted proteins for degradation through the proteasome.[58] In addition to this "classic" route for protein breakdown, ubiquitination of membrane integral proteins with one ubiquitin (monoubiquitination) directs these proteins to multivesicular bodies then to lysosomes for degradation.[59] However, lysosome-degraded proteins are thought to be deubiquitinated before import into the lysosome. Immunoblotting results showed that proteins accumulated in late endosomal/lysosomal fractions were mostly polyubiquitinated; these proteins should be degraded in proteasomes located in the cytoplasm. How these proteins are delivered to lysosomes is not clear. Mutation of NPC1 proteins not only leads to accumulation of cholesterol in late endosomal/lysosomal compartments but also results in abnormal distribution of proteases along the endocytic pathways[60] as well as leakage of cathepsins into the cytoplasm, which would lead to lysosomal dysfunction and incomplete digestion of "cargos." As a compensative response, autophagic activity would be increased. However, due to lysosomal dysfunction, LC3 and other proteins in autophagolysosomes cannot be as efficiently degraded as under normal conditions,[61,62] which leads to further increase in accumulation of undigested proteins.

Cholesterol Accumulation-Associated Autophagic-Lysosomal Dysfunction May Contribute to Neurodegeneration in Npc1$^{-/-}$ Mice

Several lines of evidence have indicated that autophagic cell death is involved in cell death that normally occurs during postnatal development in the nervous system[27] and in several neuronal degenerative diseases and animal models of these diseases.[28–30] Expression of α-synuclein with the same mutations as those found in early-onset Parkinson's disease in a cultured cell line induced massive accumulation of autophagic vacuoles and impairment of the ubiquitin-proteasome system.[63] Ultrastructural examination revealed that both apoptotic and autophagic features were present in degenerating neurons of the substantia nigra in Parkinson's disease patients.[30] In the case of AD, an earlier study reported the existence of active caspase 3 in autophagic vacuoles, which led the authors to propose that autophagy might be neuroprotective in AD.[28] However, a more recent study by Nixon and colleagues[29] demonstrated that autophagic vacuoles were abundant in degenerating neurites and were specifically colocalized with neurofibrillary tangles in perikarya. These findings support the

involvement of autophagy in neurodegeneration. *In vitro* experiments showed that trophic factor withdrawal induced Purkinje cell death with increased autophagy,[64] whereas autophagy inhibition prevented both increased vacuolation and loss of Purkinje cells. *In vivo* evidence supporting a role of autophagy in neurodegeneration also came from studies of *lurcher* mice. Selective Purkinje cell death in *lurcher* mice is caused by mutations in the δ2 glutamate receptor (GluRδ2).[65] Additional experiments demonstrated that mutations in GluRδ2 resulted in enhanced autophagy, possibly by interactions between the mutated receptors and the autophagic protein Beclin1.[65,66] These results provided strong evidence for a direct link between autophagy and Purkinje cell death in *lurcher* mice. As autophagy is generally followed by the fusion of lysosomes with autophagosomes and formation of autophagolysosomes, in which the autophagic components are degraded.[67] The beneficial or detrimental effect of autophagy may depend on the functional status of compartments downstream of the autophagic pathway. Defects in completing autophagy could result in accumulation of autophagosomes and autophagolysosomes, which could impair cell function. Furthermore, accumulation of autophagolysosomes could feedback on lysosomal function and induce lysosomal membrane permeabilization and translocation of cathepsins to the cytosol, a process implicated in cell death induced by various insults.[49,68] Release of cathepsins from lysosomes into cytosol could also initiate caspase-dependent apoptosis via activation of proapoptotic factors such as Bax, Bid, and caspases, as in the case of staurosporine-induced cell death.[22–24] Cleavage of the microtubule associated protein tau by cytosolic cathepsin D has been proposed to participate in AD pathogenesis and transport failure due to impairment in microtubule formation is postulated to contribute to accumulation of autophagosomes/autophagolysosomes in AD brain.[29]

In addition to demonstrating enhanced autophagic activity in brains of Npc1$^{-/-}$ mice, results from the present study showed an abnormal subcellular distribution of LC3-labeled autophagosomes. In contrast to the notion that autophagy is a reaction to starvation, appreciable amounts of autophagosomes existed in Purkinje cells of 8-week-old wild-type mice, suggesting that autophagy may contribute to the maintenance of normal morphology and function of neurons. This notion is supported by the recent discoveries that knocking out two critical proteins of the autophagy machinery, Atg5 and Atg7, resulted in massive neurodegeneration.[69,70] In Purkinje cells of Npc1$^{-/-}$ mice, LC3-labeled autophagosomes aggregated and colocalized with cholesterol clusters, indicating an abnormal autophagy-lysosome system. It is conceivable that cholesterol accumulation in the endosomal/lysosomal system impairs autophagosome fusion with lysosomes. It is also possible that accumulated cholesterol "traps" the autophagy machinery and other proteins in late compartments of the endocytic pathway, thereby impairing cell function. The fact that Purkinje cell in mutant mice seemed to lack classic lysosomes as observed in wild-type mice indicates an abnormal autophagic-lysosomal system in the Npc1$^{-/-}$ mice. The hypothesis that lysosomal dysfunction redirects autophagy toward cell death is supported by the finding that inhibition of lysosome fusion with autophagic vacuoles in starved cells induced an early-onset autophagic cell death followed by classic apoptosis.[71,72]

In summary, the present study presented evidence that increases in brain levels of lysosomal cathepsins B and D occurred early during postnatal development in brains of Npc1$^{-/-}$ mice, in particular in areas that exhibited early-onset neurodegeneration. Changes in lysosomal function were accompanied with relocation of ubiquitinated proteins in endosomes/lysosomes. Redistribution of these proteins may result from enhanced autophagic activity, which was demonstrated by immunoblotting and immunofluorescence analysis of LC3 and ultrastructural detection of autophagic vacuoles. These results provide the first evidence that accumulation of cholesterol alters autophagy-lysosome function and diverts this system toward neurodegeneration in NPC.

Acknowledgments

We thank Kevin Lee, Carman Rivera, Cynthia Chan, and Clara Yu for excellent technical assistance, and Dr. T. Yoshimori, National Institute of Genetics, Japan, for anti-LC3 antibodies.

References

1. Vance JE: Lipid imbalance in the neurological disorder, Niemann-Pick C disease. FEBS Lett 2006, 580:5518–5524
2. Chang TY, Reid PC, Sugii S, Ohgami N, Cruz JC, Chang CC: Niemann-Pick type C disease and intracellular cholesterol trafficking. J Biol Chem 2005, 280:20917–20920
3. Carstea ED, Morris JA, Coleman KG, Loftus SK, Zhang D, Cummings C, Gu J, Rosenfeld MA, Pavan WJ, Krizman DB, Nagle J, Polymeropoulos MH, Sturley SL, Ioannou YA, Higgins ME, Comly M, Cooney A, Brown A, Kaneski CR, Blanchette-Mackie EJ, Dwyer NK, Neufeld EB, Chang TY, Liscum L, Strauss JF, Ohno K, Zeigler M, Carmi R, Sokol J, Markie D, O'Neill RR, van Diggelen OP, Elleder M, Patterson MC, Brady RO, Vanier MT, Pentchev PG Tagle DA: Niemann-Pick C1 disease gene: homology to mediators of cholesterol homeostasis. Science 1997, 277:228–231
4. Blom TS, Linder MD, Snow K, Pihko H, Hess MW, Jokitalo E, Veckman V, Syvanen AC, Ikonen E: Defective endocytic trafficking of NPC1 and NPC2 underlying infantile Niemann-Pick type C disease. Hum Mol Genet 2003, 12:257–272
5. Garver WS, Heidenreich RA: The Niemann-Pick C proteins and trafficking of cholesterol through the late endosomal/lysosomal system. Curr Mol Med 2002, 2:485–505
6. Ory DS: Niemann-Pick type C: a disorder of cellular cholesterol trafficking. Biochim Biophys Acta 2000, 1529:331–339
7. Burns M, Duff K: Cholesterol in Alzheimer's disease and tauopathy. Ann NY Acad Sci 2002, 977:367–375
8. Liscum L: Niemann-Pick type C mutations cause lipid traffic jam. Traffic 2000, 1:218–225
9. Strittmatter WJ: Apolipoprotein E and Alzheimer's disease. Ann NY Acad Sci 2000, 924:91–92
10. Michikawa M: Cholesterol paradox: is high total or low HDL cholesterol level a risk for Alzheimer's disease? J Neurosci Res 2003, 72:141–146
11. Nixon RA, Cataldo AM, Mathews PM: The endosomal-lysosomal system of neurons in Alzheimer's disease pathogenesis: a review. Neurochem Res 2000, 25:1161–1172
12. Auer IA, Schmidt ML, Lee VM, Curry B, Suzuki K, Shin RW, Pentchev PG, Carstea ED, Trojanowski JQ: Paired helical filament tau (PHFtau)

in Niemann-Pick type C disease is similar to PHFtau in Alzheimer's disease. Acta Neuropathol (Berl) 1995, 90:547–551
13. Suzuki K, Parker CC, Pentchev PG, Katz D, Ghetti B, D'Agostino AN, Carstea ED: Neurofibrillary tangles in Niemann-Pick disease type C. Acta Neuropathol (Berl) 1995, 89:227–238
14. Love S, Bridges LR, Case CP: Neurofibrillary tangles in Niemann-Pick disease type C. Brain 1995, 118:119–129
15. Patterson MC, Pentchev PG: Niemann-Pick; type C. Neurology 1996, 46:1785–1786
16. Distl R, Meske V, Ohm TG: Tangle-bearing neurons contain more free cholesterol than adjacent tangle-free neurons. Acta Neuropathol (Berl) 2001, 101:547–554
17. Distl R, Treiber-Held S, Albert F, Meske V, Harzer K, Ohm TG: Cholesterol storage and tau pathology in Niemann-Pick type C disease in the brain. J Pathol 2003, 200:104–111
18. Cataldo AM, Paskevich PA, Kominami E, Nixon RA: Lysosomal hydrolases of different classes are abnormally distributed in brains of patients with Alzheimer disease. Proc Natl Acad Sci USA 1991, 88:10998–11002
19. Ginsberg SD, Hemby SE, Lee VM, Eberwine JH, Trojanowski JQ: Expression profile of transcripts in Alzheimer's disease tangle-bearing CA1 neurons. Ann Neurol 2000, 48:77–87
20. Callahan LM, Vaules WA, Coleman PD: Quantitative decrease in synaptophysin message expression and increase in cathepsin D message expression in Alzheimer disease neurons containing neurofibrillary tangles. J Neuropathol Exp Neurol 1999, 58:275–287
21. Bi X, Yong AP, Zhou J, Ribak CE, Lynch G: Rapid induction of intraneuronal neurofibrillary tangles in apolipoprotein E-deficient mice. Proc Natl Acad Sci USA 2001, 98:8832–8837
22. Bidère N, Lorenzo HK, Carmona S, Laforge M, Harper F, Dumont C, Senik A: Cathepsin D triggers Bax activation, resulting in selective apoptosis-inducing factor (AIF) relocation in T lymphocytes entering the early commitment phase to apoptosis. J Biol Chem 2003, 278:31401–31411
23. Johansson AC, Steen H, Ollinger K, Roberg K: Cathepsin D mediates cytochrome c release and caspase activation in human fibroblast apoptosis induced by staurosporine. Cell Death Differ 2003, 10:1253–1259
24. Cirman T, Oresic K, Mazovec GD, Turk V, Reed JC, Myers RM, Salvesen GS, Turk B: Selective disruption of lysosomes in HeLa cells triggers apoptosis mediated by cleavage of Bid by multiple papain-like lysosomal cathepsins. J Biol Chem 2004, 279:3578–3587
25. Schweichel JU, Merker HJ: The morphology of various types of cell death in prenatal tissues. Teratology 1973, 7:253–266
26. Uchiyama Y: Autophagic cell death and its execution by lysosomal cathepsins. Arch Histol Cytol 2001, 64:233–246
27. Clarke PG: Developmental cell death: morphological diversity and multiple mechanisms. Anat Embryol (Berl) 1990, 181:195–213
28. Stadelmann C, Deckwerth TL, Srinivasan A, Bancher C, Bruck W, Jellinger K, Lassmann H: Activation of caspase-3 in single neurons and autophagic granules of granulovacuolar degeneration in Alzheimer's disease: evidence for apoptotic cell death. Am J Pathol 1999, 155:1459–1466
29. Nixon RA, Wegiel J, Kumar A, Yu WH, Peterhoff C, Cataldo A, Cuervo AM: Extensive involvement of autophagy in Alzheimer disease: an immuno-electron microscopy study. J Neuropathol Exp Neurol 2005, 64:113–122
30. Anglade P, Vyas S, Javoy-Agid F, Herrero MT, Michel PP, Marquez J, Mouatt-Prigent A, Ruberg M, Hirsch EC, Agid Y: Apoptosis and autophagy in nigral neurons of patients with Parkinson's disease. Histol Histopathol 1997, 12:25–31
31. Ko DC, Milenkovic L, Beier SM, Manuel H, Buchanan J, Scott MP: Cell-autonomous death of cerebellar Purkinje neurons with autophagy in Niemann-Pick type C disease. PLoS Genet 2005, 1:81–95
32. Baudry M, Yao Y, Simmons D, Liu J, Bi X: Postnatal development of inflammation in a murine model of Niemann-Pick type C disease: immunohistochemical observations of microglia and astroglia. Exp Neurol 2003, 184:887–903
33. Kabeya Y, Mizushima N, Ueno T, Yamamoto A, Kirisako T, Noda T, Kominami E, Ohsumi Y, Yoshimori T: LC3, a mammalian homologue of yeast Apg8p, is localized in autophagosome membranes after processing. EMBO J 2000, 19:5720–5728
34. Bornig H, Geyer G: Staining of cholesterol with the fluorescent antibiotic "filipin." Acta Histochem 1974, 50:110–115
35. Bednarski E, Ribak CE, Lynch G: Suppression of cathepsins B and L causes a proliferation of lysosomes and the formation of meganeurites in hippocampus. J Neurosci 1997, 17:4006–4021
36. Liaudet-Coopman E, Beaujouin M, Derocq D, Garcia M, Glondu-Lassis M, Laurent-Matha V, Prebois C, Rochefort H, Vignon F: Cathepsin D: Newly discovered functions of a long-standing aspartic protease in cancer and apoptosis. Cancer Lett 2006, 237:167–179
37. Follo C, Castino R, Nicotra G, Trincheri NF, Isidoro C: Folding, activity and targeting of mutated human cathepsin D that cannot be processed into the double-chain form. Int J Biochem Cell Biol 2007, 39:638–649
38. Jäger S, Bucci C, Tanida I, Ueno T, Kominami E, Saftig P, Eskelinen EL: Role for Rab7 in maturation of late autophagic vacuoles. J Cell Sci 2004, 117:4837–4848
39. Gutierrez MG, Munafo DB, Beron W, Colombo MI: Rab7 is required for the normal progression of the autophagic pathway in mammalian cells. J Cell Sci 2004, 117:2687–2697
40. Mariño G, Lopez-Otin C: Autophagy: molecular mechanisms, physiological functions and relevance in human pathology. Cell Mol Life Sci 2004, 61:1439–1454
41. Keller JN, Dimayuga E, Chen Q, Thorpe J, Gee J, Ding Q: Autophagy, proteasomes, lipofuscin, and oxidative stress in the aging brain. Int J Biochem Cell Biol 2004, 36:2376–2391
42. Tanida I, Tanida-Miyake E, Ueno T, Kominami E: The human homolog of Saccharomyces cerevisiae Apg7p is a protein-activating enzyme for multiple substrates including human Apg12p, GATE-16, GABARAP, and MAP-LC3. J Biol Chem 2001, 276:1701–1706
43. Gozuacik D, Kimchi A: Autophagy as a cell death and tumor suppressor mechanism. Oncogene 2004, 23:2891–2906
44. German DC, Liang CL, Song T, Yazdani U, Xie C, Dietschy JM: Neurodegeneration in the Niemann-Pick C mouse: glial involvement. Neuroscience 2002, 109:437–450
45. Lynch G, Bi X: Lysosomes and brain aging in mammals. Neurochem Res 2003, 28:1725–1734
46. Bi X, Haque TS, Zhou J, Skillman AG, Lin B, Lee CE, Kuntz ID, Ellman JA, Lynch G: Novel cathepsin D inhibitors block the formation of hyperphosphorylated tau fragments in hippocampus. J Neurochem 2000, 74:1469–1477
47. Bednarski E, Lynch G: Cytosolic proteolysis of tau by cathepsin D in hippocampus following suppression of cathepsins B and L. J Neurochem 1996, 67:1846–1855
48. Bi X, Zhou J, Lynch G: Lysosomal protease inhibitors induce meganeurites and tangle-like structures in entorhinohippocampal regions vulnerable to Alzheimer's disease. Exp Neurol 1999, 158:312–327
49. Yang AJ, Chandswangbhuvana D, Margol L, Glabe CG: Loss of endosomal/lysosomal membrane impermeability is an early event in amyloid Aβ1-42 pathogenesis. J Neurosci Res 1998, 52:691–698
50. Burns M, Gaynor K, Olm V, Mercken M, LaFrancois J, Wang L, Mathews PM, Noble W, Matsuoka Y, Duff K: Presenilin redistribution associated with aberrant cholesterol transport enhances β-amyloid production in vivo. J Neurosci 2003, 23:5645–5649
51. Pagano RE: Endocytic trafficking of glycosphingolipids in sphingolipid storage diseases. Philos Trans R Soc Lond B Biol Sci 2003, 358:885–891
52. Lebrand C, Corti M, Goodson H, Cosson P, Cavalli V, Mayran N, Faure J, Gruenberg J: Late endosome motility depends on lipids via the small GTPase Rab7. EMBO J 2002, 21:1289–1300
53. Choudhury A, Dominguez M, Puri V, Sharma DK, Narita K, Wheatley CL, Marks DL, Pagano RE: Rab proteins mediate Golgi transport of caveola-internalized glycosphingolipids and correct lipid trafficking in Niemann-Pick C cells. J Clin Invest 2002, 109:1541–1550
54. Mayran N, Parton RG, Gruenberg J: Annexin II regulates multivesicular endosome biogenesis in the degradation pathway of animal cells. EMBO J 2003, 22:3242–3253
55. Bi X, Liu J, Yao Y, Baudry M, Lynch G: Deregulation of GSK-3β and NF-κB is associated with neurodegeneration in $Npc1^{-/-}$ mouse brain. Am J Pathol 2005, 167:1081–1092
56. Bijur GN, Jope RS: Glycogen synthase kinase-3β is highly activated in nuclei and mitochondria. Neuroreport 2003, 14:2415–2419
57. Zhu JH, Guo F, Shelburne J, Watkins S, Chu CT: Localization of phosphorylated ERK/MAP kinases to mitochondria and autophagosomes in Lewy body diseases. Brain Pathol 2003, 13:473–481
58. Ciechanover A: Intracellular protein degradation: from a vague idea thru the lysosome and the ubiquitin-proteasome system and onto

human diseases and drug targeting. Cell Death Differ 2005, 12:1178–1190
59. d'Azzo A, Bongiovanni A, Nastasi T: E3 ubiquitin ligases as regulators of membrane protein trafficking and degradation. Traffic 2005, 6:429–441
60. Jin LW, Maezawa I, Vincent I, Bird T: Intracellular accumulation of amyloidogenic fragments of amyloid-β precursor protein in neurons with Niemann-Pick type C defects is associated with endosomal abnormalities. Am J Pathol 2004, 164:975–985
61. Tanida I, Minematsu-Ikeguchi N, Ueno T, Kominami E: Lysosomal turnover, but not a cellular level, of endogenous LC3 is a marker for autophagy. Autophagy 2005, 1:84–91
62. Koike M, Shibata M, Waguri S, Yoshimura K, Tanida I, Kominami E, Gotow T, Peters C, von Figura K, Mizushima N, Saftig P, Uchiyama Y: Participation of autophagy in storage of lysosomes in neurons from mouse models of neuronal ceroid-lipofuscinoses (Batten disease). Am J Pathol 2005, 167:1713–1728
63. Stefanis L, Larsen KE, Rideout HJ, Sulzer D, Greene LA: Expression of A53T mutant but not wild-type α-synuclein in PC12 cells induces alterations of the ubiquitin-dependent degradation system, loss of dopamine release, and autophagic cell death. J Neurosci 2001, 21:9549–9560
64. Florez-McClure ML, Linseman DA, Chu CT, Barker PA, Bouchard RJ, Le SS, Laessig TA, Heidenreich KA: The p75 neurotrophin receptor can induce autophagy and death of cerebellar Purkinje neurons. J Neurosci 2004, 24:4498–4509
65. Yue Z, Horton A, Bravin M, DeJager PL, Selimi F, Heintz N: A novel protein complex linking the delta 2 glutamate receptor and autophagy: implications for neurodegeneration in lurcher mice. Neuron 2002, 35:921–933
66. Selimi F, Lohof AM, Heitz S, Lalouette A, Jarvis CI, Bailly Y, Mariani J: Lurcher GRID2-induced death and depolarization can be dissociated in cerebellar Purkinje cells. Neuron 2003, 37:813–819
67. Mizushima N, Ohsumi Y, Yoshimori T: Autophagosome formation in mammalian cells. Cell Struct Funct 2002, 27:421–429
68. Paquet C, Sane AT, Beauchemin M, Bertrand R: Caspase- and mitochondrial dysfunction-dependent mechanisms of lysosomal leakage and cathepsin B activation in DNA damage-induced apoptosis. Leukemia 2005, 19:784–791
69. Hara T, Nakamura K, Matsui M, Yamamoto A, Nakahara Y, Suzuki-Migishima R, Yokoyama M, Mishima K, Saito I, Okano H, Mizushima N: Suppression of basal autophagy in neural cells causes neurodegenerative disease in mice. Nature 2006, 441:885–889
70. Komatsu M, Waguri S, Chiba T, Murata S, Iwata J, Tanida I, Ueno T, Koike M, Uchiyama Y, Kominami E, Tanaka K: Loss of autophagy in the central nervous system causes neurodegeneration in mice. Nature 2006, 441:880–884
71. González-Polo RA, Boya P, Pauleau AL, Jalil A, Larochette N, Souquere S, Eskelinen EL, Pierron G, Saftig P, Kroemer G: The apoptosis/autophagy paradox: autophagic vacuolization before apoptotic death. J Cell Sci 2005, 118:3091–3102
72. Boya P, Gonzalez-Polo RA, Casares N, Perfettini JL, Dessen P, Larochette N, Metivier D, Meley D, Souquere S, Yoshimori T, Pierron G, Codogno P, Kroemer G: Inhibition of macroautophagy triggers apoptosis. Mol Cell Biol 2005, 25:1025–1040